Tide-related changes in mRNA abundance of aromatase and estrogen receptors in the ovary and brain of the threespot wrasse *Halichoeres trimaculatus*

Dae-Ju Oh[1], Sung-Pyo Hur[2], Selma Bouchekioua[3], Yuki Takeuchi[3], Shingo Udagawa[3], Neelakanteswar Aluru[5], Yong-Ju Park[3], Ji-Gweon Park[1], Se-Jae Kim[4], Thomas W. Moon[6], Mathilakath M. Vijayan[7], Akihiro Takemura[3]

[1]Jeju Biodiversity Research Institute, Jeju Technopark, 338 Shinryedong-ro, Namwon-eup, Seogwipo, 63608, Republic of Korea

[2]Jeju International Marine Science Research & Logistics Center, Korea Institute of Ocean Science & Technology, 2670, Iijudong-ro, Gujwa-eup, Jeju, 63349, Republic of Korea

[3]Department of Chemistry, Biology and Marine Science, Faculty of Science, University of the Ryukyus, 1 Senbaru, Nishihara, Okinawa 903-0213, Japan

[4]Department of Biology, Jeju National University, 102 Jejudaehak-ro, Jeju, 63243, Republic of Korea

[5]Biology Department, Woods Hole Oceanographic Institution, Woods Hole, Massachusetts, MA 02543, USA

[6]Department of Biology, University of Ottawa, Ottawa, Ontario ON K1N 6N5, Canada

[7]Department of Biological Sciences, University of Calgary, 2500 University Drive NW, Calgary AB T2N 1N4, Canada

Running title: Tidal changes in ER and aromatase transcripts

*Corresponding author
Sung-Pyo Hur
Jeju International Marine Science Research & Logistics Center, Korea Institute of Ocean Science & Technology, 2670, Iijudong-ro, Gujwa-eup, Jeju, Korea
Tel: +82-64-798-6107, Fax: +82-798-6039
E-mail: hursp@kiost.ac.kr

ABSTRACT

The threespot wrasse (*Halichoeres trimaculatus*; Family Labridae) is a common coral reef species of the Indo-Pacific Ocean. Given that this species spawns daily at high tide (HT), we hypothesized that endocrine changes in relation to gonadal development are synchronized with the tidal cycle. To test this, we examined the transcript abundance of two cytochrome P450 aromatases (*cyp19a* and *cyp19b*) and two estrogen receptors (*er*α and *er*β) in the ovary and brain of this species in response to tidal change. When fish were collected around four tidal points [low tide (LT), flood tide (FT), high tide (HT), and ebb tide (ET)], gonadosomatic index and oocyte diameter increased around HT and FT, respectively. Ovulatory follicles were observed in ovaries around HT. Real-time quantitative polymerase-chain reaction revealed that mRNA abundance of *cyp19a* and *er*α, but not *er*β, in the ovary increased around ET and HT, respectively. On the other hand, mRNA levels of *cyp19b* in the forebrain were significantly higher around FT. Increases of *er*α and *er*β mRNA abundance around FT were observed in all areas of the brain and the midbrain, respectively. The changes in mRNA abundance of key genes involved in reproduction at specific tidal cycles, along with the development of the vitellogenic oocytes in the ovary, support our hypothesis that synchronization of endocrine changes to the tidal periodicity plays a role in the gonadal development of this species. We hypothesize that conversion of testosterone to E2 in the brain may be associated with the spawning behavior given that the wrasse exhibits group spawning with a territory-holding male around HT.

Keywords: aromatase, brain, estrogen receptor, ovary, tide, wrasse

Introduction

Estradiol-17β (E2) plays an important role in reproductive processes including oogenesis, vitellogenesis, and gonadotropin regulation in female fish (Nelson and Habibi 2013). This sex steroid is converted mainly from testosterone through catalytic activity by aromatases (P450arom) that belong to the cytochrome P450 (CYP19) superfamily and are differentially expressed in the ovary (named CYP19A1 or P450aromA) and the brain (named CYP19A2/P450aromBb). They are derived from the separated gene loci of *CYP19a1a* and *CYP19a1b*, respectively (Blázquez and Piferrer, 2004; Tchoudakova and Callard, 1998; Tchoudakova et al., 2001). It was reported in certain fishes that mRNA transcript abundance of *cyp19a1a* and *cyp19a1b* are positively correlated with aromatase activity and plasma E2 levels during ovarian recrudescence, suggesting that these genes are involved in female reproduction through E2 synthesis in the brain and ovary during the breeding season (Chaube et al., 2015; Li et al., 2007). The brain-derived E2 is considered to play a role in neuronal and/or glial signaling in relation to reproduction (Hojo et al., 2003; Holloway and Clayton, 2001; Zwain and Yen, 1999).

E2 action in target tissues is mediated by cytosolic estrogen receptors (ERs), which belong to the nuclear receptor superfamily and are made up of distinct subtypes including ERα and ERβ (Hawkins et al. 2000). An additional ER subtype (named ERβ2 or ERγ) was also reported in ray-finned fish species (Choi and Habibi, 2003; Hawkins et al., 2000; Ma et al. 2000; Menuet et al., 2002; Nagler et al., 2007). In some fish species including the Korean rockfish (*Sebastes schlegeli*), the rainbow trout (*Oncorhynchus mykiss*), and the orange-spotted grouper (*Epinepherus coioides*), the mRNA abundance of *erα1*, but not *erβ1* and *erβ2*, is highly expressed in the liver and positively correlated with plasma levels of E2 and vitellogenin (Chen et al., 2011; Mu et al., 2013; Nagler et al., 2012). On the other hand, E2

78 treatment resulted in up-regulation of three ER subtypes (*erα*, *erβ1*, and *erβ2*) in the ovary of
79 goldfish *Carassius auratus* (Nelson et al., 2007). Down-regulation of *erα1* and *er2b* was
80 observed in the ovary of the fathead minnow (*Pimephales promelas*) in relation to exposure to
81 exogenous E2 (Filby et al., 2006). It, therefore, appears that ERs are differently expressed
82 among tissues in accordance with gonadal development.

83 Wrasses belong to the Family Labridae and are largely distributed in shallow waters with
84 rocky and sandy bottoms from tropical to temperate waters. Most wrasses are known to be
85 protogynous hermaphrodites with a haremic mating system and to spawn daily during the
86 breeding season (Ross, 1983; Warner, 1982). A diurnal pattern of ovarian development is
87 reported in certain wrasses (Matsuyama et al., 1998, 2002; Takemura et al., 2008).
88 Interestingly, tidal cycle seems to be superimposed on daily spawning in tropical wrasses
89 (Colin and Bell, 1991; Hoffman and Grau, 1989; Ross, 1983; Takemura et al., 2008; Warner,
90 1982). For instance, in the ovary of the threespot wrasse (*Halichoeres trimaculatus*),
91 vitellogenic oocyte development is synchronized to the tidal cycle and ovulation/spawning
92 occurs around daytime high tide (Takemura et al., 2008). Since E2 synthesis is also related to
93 the developmental pattern of vitellogenic oocytes in the ovary (Takemura et al., 2008), we
94 hypothesized that the expression of steroidogenic enzymes and steroid hormone receptors will
95 also change in relation to the tidal cycle. The aim of the present study was to investigate
96 changes in the mRNA abundance of *ER* and *CYP19* genes in the ovary and brain of the
97 threespot wrasse during the tidal cycle in Okinawan waters. Mature females were collected
98 around four tidal points [low tide (LT), flood tide (FT), high tide (HT), and ebb tide (ET)] and
99 mRNA transcript abundance of *CYP19* paralogs (*cyp19a* and *cyp19b*) and *ER* paralogs (*erα*
100 and *erβ*) were assessed using real-time quantitative polymerase-chain reaction (qPCR).
101
102 **Materials and methods**

Animals

Mature females were collected in coral reefs around Sesoko Island, Okinawa, Japan, during the low tide (LT), flood tide (FT), high tide (HT), and ebb tide (ET) in July. Fish were anesthetized with 2-phenoxyethanol (Kanto Chemical, Tokyo, Japan). After recording body mass and total length, blood was taken from the caudal vein using a 1-ml heparinized syringe, centrifuged at 10,000 *g* for 10 min to obtain plasma, and then frozen at –30 ºC until analyzed. Fish were then euthanized by decapitation. The whole brain was removed, divided into three parts – forebrain, midbrain and hindbrain (Fig. 1) – and kept frozen at –80 ºC until RNA extraction. Ovary was also removed from the body cavity and weighed and pieces of this tissue were frozen at –80 ºC for RNA extraction or fixed in Bouin's solution for histological observation. Gonadosomatic index (GSI) was calculated using the following equation; GSI = (gonad mass/body mass) × 100.

All experiments were conducted in compliance with both the Animal Care and Use Committee guidelines of the University of the Ryukyus and the Regulations for the Care and Use of Laboratory Animals in Japan.

Histological observation and oocyte diameter measurement

The fixed ovary samples were dehydrated with an ethanol series, permeated with xylene, and then embedded in histoparaffin (Paraplast plus; Sigma-Aldrich, St. Louis, MO, USA). The embedded ovaries were serially sectioned at 5 μm thickness and stained with Delafield's hematoxylin-eosin for microscopic observation. Development of vitellogenic oocytes was determined by measuring oocyte diameter of the most developed oocytes (n = 30) in each

ovary. Oocytes were classified according to Hoque et al. (1998) into the following stages: peri-nucleolus stage (PNS), oil-droplet stage (ODS), primary yolk stage (PYS), secondary yolk stage (SYS), tertiary yolk stage (TYS), migratory nucleus stage (MNS), and maturation stage (MS). Post-ovulatory follicle (POF) were classified as described previously (Matsuyama et al., 1990).

Measurement of steroid hormone levels

Plasma levels of E2 were measured by enzyme immunosorbent assay (EIA), according to the method of Asahina et al. (1995). Briefly, plasma samples (30 µl) were extracted three times with 1 ml diethyl ether (Kanto Chemical) and vortexed for 1 min. Diethyl ether fractions containing steroid hormones were transferred to a clean assay tube and subjected to centrifugal evaporation (VEC-310, EYELA, Tokyo, Japan). Then, 120 µl 50 mM borate buffer (pH 7.8, containing 0.5% bovine serum albumin) was added to each tube and vortexed for 1 min.

Each well of a 96-well plate (AFC Techno Glass, Funabashi, Japan) was coated with 100 µl (4.6 µg/ml) of goat anti-rabbit IgG (Jackson Immunoresearch, PA, USA) in 50 mM carbonate buffer (pH 9.6) and incubated overnight at 4 ^{o}C. The well were washed three times with 10 mM phosphate-buffer saline (PBS) containing 0.05% Tween (PBS-Tween) using an ImmunoWash 1575 microplate washer (Bio-Rad Laboratories, Hercules, CA, USA). The assay was performed in a total volume of 120 µl, which consisted of 40 µl E2 standards (Sigma-Aldrich; 12.8 to 0.025 ng/ml) or plasma samples, 40 µl diluted steroid labeled with horseradish peroxidase (Cosmo-Bio, Tokyo, Japan), and 40 µl rabbit anti-E2 antibody (Cosmo-Bio).

Incubation was done overnight at 4 ^{o}C. After washing three times with PBS-Tween, 100

153 μl 100 mM citrate buffer (pH 4.5) containing 0.01% *o*-phenylenediamine dihydrochloride
154 (Sigma-Aldrich) and 0.04% H_2O_2 was added to each well. After leaving the plate at room
155 temperature for 30 min, 25 μl 4 N H_2SO_4 was added to each well to stop the reaction.
156 Absorbance of each well was measured at 490 nm using a 550 microplate reader (BioRad).
157 The intra- and inter-assay coefficients of variations at the 50% binding point were 5% (n = 4,
158 duplicate) and 8% (n = 4, duplicate), respectively, for E2.
159
160 RNA extraction and cDNA synthesis
161
162 Total RNA was extracted using TRI-reagent (Molecular Research Center, Cincinnati, OH,
163 USA), according to the manufacturer's instructions. After ovarian or brain samples (50 to 100
164 mg) were homogenized in 1 ml TRI-reagent, 0.2 ml chloroform was added to the homogenate
165 and mixed vigorously. The mixture was stored at room temperature for 15 min and
166 centrifuged at 12,000 *g* for 15 min at 4 °C. The aqueous phase was transferred to a fresh tube
167 and RNA was precipitated from the aqueous phase by mixing in 0.5 ml isopropanol. Samples
168 were stored at room temperature for 10 min and centrifuged at 12,000 *g* for 8 min at 4 °C.
169 After removal of the supernatant, RNA pellets were washed twice with 80%
170 diethylpyrocarbonate (DEPC)-ethanol and then centrifuged at 7,500 *g* for 5 min at 4 °C. After
171 the ethanol was removed, RNA pellets were briefly air-dried for 5 min at room temperature
172 and dissolved in DEPC-H_2O. Absorbance was measured at 260 nm and 280 nm to calculate
173 the quantity and purity of RNA.
174 The first strand cDNAs were synthesized from 1 μg total RNA using ImProm-II™
175 Reverse Transcription System (Promega, Madison, WI, USA) according to manufacturer's
176 instructions. After incubation at 70 °C for 5 min, 25 °C for 5 min, and 42 °C for 60 min,
177 enzymatic activity was inactivated by heating at 72 °C for 15 min. After cDNA synthesis, the

reaction mixture was diluted to a final volume of 100 µl by adding 80 µl of nuclease-free water.

mRNA transcript abundance of ER and aromatase genes

The *cyp19a*, *cyp19b*, *erα*, and *erβ* cDNAs of the threespot wrasse were amplified by PCR reaction with primer sets (Table 1) designed from those of the bambooleaf wrasse (*Pseudolabrus japonicus*) (GenBank Accession Numbers: DQ298134, DQ298133, DQ298135, and DQ298136, respectively). PCR was performed using 30 cycles each of denaturation (45 s at 94 °C), annealing (45 s at 53 °C), and extension (1 min at 72 °C). PCR products were cloned into the pGEM-T easy vector (Promega) and sequenced. A phylogenetic tree was constructed by the JTT method with the PRODIST program from the PHYLIP package (ver. 3.63, J. Felsenstein, University of Washington, Seattle, WA, USA). One thousand bootstrap trials were run using the neighbor-joining method. The CONSENSE program of PHYLIP was used to construct a strict consensus tree.

The mRNA abundance of *er*s and *cyp19*s in tissues were analyzed using the ABI Prism 7000 (Thermo Fisher Scientific, Waltham, MA, USA). Primer sets of *er*s, *cyp19*s, and *β-actin* for qPCR analysis were designed to anneal to a region that included the exon/intron boundaries of each gene to eliminate amplification from genomic DNA (Table 1). The length of the amplicon was kept as close as possible to 100-200 bp and the melting temperature of the primers was set at 57-60 ºC. Each PCR reaction mix contained 10 µl SYBR *Premix Ex taq* (Takara, Otsu, Japan), 0.4 µl forward primer and 0.4 µl reverse primer (10 µM) and 2 µl cDNA template, which was adjusted to a total volume of 20 µl by adding distilled water. The initial 1 min denaturation was followed by 40 cycles of denaturation for 5 s at 95 °C, and annealing and extension for 1 min at 60 °C. To ensure specificity, a dissociation curve

analysis was performed by slowly raising the temperature of the sample from 60 °C to 95 °C. A series of 10-fold dilutions of plasmid DNA encoding *er*s, *cyp19*s, and *β-actin* were prepared and included in each amplification reaction to generate a standard curve. These curves showed a single amplified product and the absence of primer-dimer formation (data not shown). The abundance level of each transcript was calculated relative to the internal control (*β-actin*).

Statistics

All the data are expressed as means ± standard error of the mean (SEM). Differences between the mRNA transcript levels of *cyp19a*, *cyp19b*, *erα*, and *erβ*, plasma levels of E2, as well as GSI and oocyte diameters with tidal change were determined by one-way analysis of variance (ANOVA), followed by LSD-Duncan test, using SPSS for windows software. A significant level at $P < 0.05$ was accepted.

Results

The deduced amino acid sequences of CYP19s (GenBank accession No. LR35003 for CYP19a, LR35004 for CYP19b) and ERs (KT210387 for ERα , and KT210388 for ERβ) of the threespot wrasse were compared with those of both teleost and other vertebrate CYP19s and ERs. A phylogenetic analysis clearly clusters the CYP19a and CYP19b of the threespot wrasse with those of other seawater teleost fish and with the appropriate teleost CYP19a and teleost CYP19b orthologs, respectively (Fig. 2). Similarly, ERα and ERβ of this species were orthologous to teleost ERs (Fig. 3).

Reproductive parameters of the female threespot wrasse were compared among the four

tidal points (Fig. 4). High values of GSI and oocyte diameter (vitellogenic oocytes) were recorded around HT (Fig. 4a) and FT (Fig. 4b), respectively. Plasma E2 levels significantly increased around LT (Fig. 4c). Oocytes at vitellogenic stages were observed in all the ovaries collected around four tidal points. Ovaries around HT, but not at other tidal points, contained POF and ovulated eggs (data not shown).

Transcript levels of *cyp19a* (ovary) or *cyp19b* (brain), *erα*, and *erβ* genes were measured in the ovary (Fig. 5) and brain (Fig. 6). In the ovary, mRNA abundance of *cyp19a* significantly increased from LT to ET (Fig. 5a), while that of *erα*, but not that of *erβ*, increased significantly around HT (Fig. 5b). Abundance of *cyp19b* mRNA significantly increased around FT in the forebrain, but not in the midbrain and hindbrain (Fig. 6). Abundance of *erα* mRNA was significantly higher around FT in three parts of the brain, while the *erβ* mRNA level was significantly higher at FT but only in the midbrain.

Discussion

In the present study, we cloned and sequenced cDNAs of two cytochrome P450 aromatases and two estrogen receptors of the threespot wrasse, and showed that they were phylogenetically related to those of other fishes. It was reported that ray-finned fish species (Actinopterygii) has at least three distinct subtypes, including ERα, ERβ-I (ERγ), and ERβ-II (Choi and Habibi, 2003; Halm et al., 2004; Hawkins et al., 2000; Ma et al., 2000; Menuet et al., 2004; Nagler et al., 2007; Tchoudakova et al., 1999). ERβ cloned in the present study seems to share identity with ERβ2 (ERβ-II) because it is included in the subclade of ERβ2, but not ERβ1, of the European sea bass (*Dicentrarchus labrax*) (Halm et al., 2004).

Our results demonstrate that the spawning of the threespot wrasse occurs at HT as evidenced by the higher GSI at this time and the presence of POF in the ovary during ET. This

supports the hypothesis that this wrasse species is a tidal spawner with high tide preference as we previously reported (Takemura et al., 2008). A similar spawning rhythmicity with high tide preference was also reported in many tropical wrasses (Colin and Bell, 1991; Ross, 1983; Warner, 1982). Our previous study revealed histologically that a clutch of vitellogenic oocytes at the tertiary yolk stage develops daily toward HT and completes the process of late vitellogenesis to final oocyte maturation within a short time period (3 h) between FT and HT (Takemura et al., 2008). Therefore, it is likely that endocrine changes triggering the final process of oocyte development occur rapidly in the ovary and brain in accordance with the tidal cycle, and repeated at regular tidal intervals (12.4 h). In support of this, plasma E2 levels increased at LT and this was followed by an increased oocyte diameter in a clutch of developing oocytes at FT. This result implies that vitellogenin synthesis in the liver occurs in response to elevated E2 at LT, which then gets incorporated into the developing oocytes. Since it was reported that plasma E2 levels peak around a period of ET (Takemura et al., 2008), there seems to be 3-h difference in a E2 peak between the two studies. This may be partially due to the rapid progress of oocyte development with tide, especially given that tide is a progressive change repeated at an interval of 12.4 h and there is only a 3-h difference between ET and LT.

Changes in P450arom enzymatic activities in the ovary play an important role in regulating the gonadal production of E2 during reproduction and development (Chang et al., 1997). Since E2 is positively correlated with stimulation of vitellogenin synthesis in hepatocytes (Nagahama, 1994), it is considered that changes in P450arom reflect the process of vitellogenesis in the ovary. Positive relationship between P450arom change and plasma E2 levels were reported in fishes, including the red-spotted grouper (*E. akaara*), where aromatase activities in the ovary peak during the breeding season when plasma E2 levels were high (Li et al., 2007). This relationship was also confirmed by treatment with an aromatase inhibitor

278 Fadrozole, which decreased plasma E2 levels in the female coho salmon (*O. kisutch*) (Afonso
279 et al., 1999). Molecular-based studies have also demonstrated a similar relationship between
280 *cyp19a* and vitellogenesis (Chang et al., 2005; Villeneuve et al., 2006; Rasheeda et al., 2010).
281 The present study showed a steady increase of *cyp19a* mRNA abundance in the ovary of the
282 threespot wrasse from LT through ET. This pattern seemed to be different from the
283 abovementioned reports (Chang et al., 2005; Villeneuve et al., 2006; Rasheeda et al., 2010)
284 showing seasonal changes in *cyp19a* mRNA abundance in the ovary of fish species with
285 synchronous or group-synchronous oocyte development (Wallace and Selman, 1981). Since
286 our previous study revealed rapid development of a clutch of larger vitellogenic oocytes (the
287 first clutch) and existence of smaller vitellogenic oocytes (the second or subsequent clutches)
288 in the ovary (Takemura et al., 2008), the present results on the expression pattern of *cyp19a*
289 mRNA abundance may be due to a rapid rise of aromatase activity in relation to the second
290 clutch of vitellogenic oocytes in an ovary.

291 ERs are cytosolic transducers of the estrogen signal in cells or neurons of target tissues.
292 Therefore, the magnitude and pattern of their mRNA abundance likely reflects potential
293 function and regulation (Nagler et al., 2012). The present study revealed that the abundance of
294 *erα* mRNA in the ovary increased around HT, while that of *erβ* mRNA did not change
295 throughout the tidal cycle. This result implies that *erα*, but not *erβ*, may be playing a role in
296 transducing the estrogen signal linked with periodical tidal change. It was reported in the
297 largemouth bass (*Micropterus salmoides*) that abundance of *erα* mRNA in the liver increased
298 in association with the increased abundance of vitellogenin mRNA in the liver and E2 levels
299 in circulation, while mRNA abundance of three *er*s (*erα*, *erβ*, *erγ*) in the ovary increased
300 during the early oocyte development and prior to the increases in plasma E2 levels (Sabo-
301 Attwood et al., 2004). In the rainbow trout, the mRNA abundance of *erα* in the liver and *erβ*s
302 in the ovary are thought to be related to the process of vitellogenin synthesis and the

303 preparation and growth of early follicles, respectively (Nagler et al., 2012). In this case,
304 however, peak *erα2* mRNA abundance was found during the late vitellogenic phase,
305 suggesting that this ER subtype plays a role in the final phase of ovarian growth in this
306 species (Nagler et al., 2012). In this regard, Nagler et al. (2012) proposed that in response to
307 an increase in E2 toward the final phase of ovarian growth, *erα2* plays a signaling role in the
308 upregulation of gonadotropin receptors in the granulosa cells, and this is responsible for
309 shutting down vitellogenin uptake through a reduction in the cycling of vitellogenin receptors
310 to the oocyte plasma membrane. Unlike yearly and synchronous ovarian growth seen in trout
311 (Wallace and Selman, 1981), a clutch of vitellogenic oocytes develops toward HT in the
312 threespot wrasse. Consequently, *erα* may be related to a rapid growth of early follicles
313 following ovulation and spawning around HT. Conversely, it is more likely that this increase
314 in *erα* accelerates the process of vitellogenesis to final oocyte maturation in a clutch of
315 oocytes facing ovulation during HT, but this remains to be tested.

316 Several reports have demonstrated reproduction-related changes in mRNA abundance of
317 *cyp19a1b* in the brain of teleost fishes (Chaube et al., 2015; Hoffman et al., 2013; Kazeto and
318 Trant, 2005; Li et al., 2007; Rasheeda et al., 2010). In the brain of the female stinging catfish
319 (*Heteropneustes fossilis*), *cyp19a1b* increased during the resting phase and preparatory phase
320 and subsequently decreased during the prespawning and spawning phase (Chaube et al., 2015;
321 Rasheeda et al., 2010). On the contrary, aromatase activity increased in the brain of the red-
322 spotted grouper during the breeding season (Li et al., 2007). Also, an increase in the transcript
323 abundance of *cyp19a2* was found in the brain and pituitary of the channel catfish (*Ictalurus*
324 *punctatus*) prior to spawning (Kazeto and Trant, 2005). These results suggest that *cyp19a1b*
325 mRNA expressions in the brain of fish show diverse patterns among species and this may be
326 partially related to their respective reproductive strategies. The present study revealed an
327 increase in *cyp19b* mRNA abundance in the forebrain, but not in the midbrain or hindbrain, of

328 the threespot wrasse during FT. Higher abundance of *cyp19b* mRNA in the telencephalon has
329 been reported in the channel catfish (Kazeto and Trant, 2005). *In situ* hybridization analysis
330 has also demonstrated a strong signal for *cyp19b* mRNA in the telencephalon of stinging
331 catfish, although high transcript levels were also observed in the lateral hypothalamus and
332 medulla oblongata (Chaube et al., 2015). The brain regions, including the ventral
333 telencephalon and hypothalamus, are involved in reproductive activity and sexual behavior,
334 and hormones, including gonadotropin-releasing hormones, vasotocin and dopamine play a
335 role in modulating these responses (Chaube et al., 2015). Since the forebrain mainly contains
336 the telencephalon (Fig. 1), this part of the wrasse brain may be involved in regulating the
337 tidal-related reproduction of this species based on changes in aromatase activity. In the
338 African cichlid fish (*Astatotilapia burtoni*), treatment with E2 increased aggression
339 (O'Connell and Hofmann, 2012), while an aromatase inhibitor abolished this aggressive
340 behaviour (Huffman et al., 2013), suggesting that local conversion from testosterone to E2 by
341 aromatase in the brain is necessary for displaying such behavior (McEwen, 1981). A similar
342 action of aromatase may occur in the brain of the threespot wrasse, since this hermaphroditic
343 labrid species exhibits group spawning with a territory-holding male (Suzuki et al., 2010).
344 Concomitant with an increase in *cyp19b*, the mRNA abundance of *er*s in the brain also
345 increased around FT. Since *erα* was highly expressed in the forebrain, midbrain, and
346 hindbrain as well as *erβ* in the midbrain, we propose that targets of E2 in the brain are likely
347 to be located to neurons and cells in these areas.
348 It is concluded that fundamental roles of these genes in the ovary and brain of the
349 threespot wrasse are equivalent to those of teleost fishes studied so far and tidal cycle is
350 superimposed on processes of gonadal development. In this regard, it was reported that
351 hydrostatic pressure is an important cue to stimulate the hypothalamic-pituitary-gonadal

(HPG) axis (Takemura et al., 2012). Further studies would be needed to clarify how the HPG axis is influenced by tidal stimuli in fish.

Acknowledgements

This study was supported partially by the 21st Century COE program "The Comprehensive Analyses on Biodiversity in Coral Reef and Island Ecosystems in Asian and Pacific Regions" from the Ministry of Education, Culture, Sports, Science and Technology, Japan, JSPS KAKENHI Grant number 16H05796, and the Natural Sciences and Engineering Research Council (NSERC, Canada) Discovery Grant program. The technical assistance rendered by Dr. Morita and Ms. McGuire is gratefully acknowledged.

References

Afonso LOB, Iwama GK, Smith J, Donaldson EM (1999) Effects of the aromatase inhibitor Fadrozole on plasma sex steroid secretion and oocytematuration in female coho salmon (*Oncorhynchus kisutch*) during vitellogenesis. Fish Physiol Biochem **20**: 231–241

Asahina K, Kambegawa A, Higashi T (1995) Development of a microtiter plate enzyme-linked immunosorbent assay for 17α,20β,21-trihydroxy-4-pregnen-3-one, a teleost gonadal steroid. Fisheries Sci **61**: 491–494

Blázquez M, Piferrer F (2004) Cloning, sequence analysis, tissue distribution, and sex-specific expression of the neural form of P450 aromatase in juvenile sea bass (*Dicentrarchus labrax*). Mol Cell Endocrinol **219**: 83–94

Chang XT, Kobayashi T, Kajiura H, Nakamura M Nagahama Y (1997) Isolation and characterization of the cDNA encoding the tilapia (*Oreochromis niloticus*) cytochrome P450 aromatase (P450arom): changes in P450arom mRNA, protein, and enzyme activity in ovarian follicles during oogenesis. J Mol Endocrinol **18**: 57-66

377 Chang X, Kobayashi T, Senthilkumaran B, Kobayashi-Kajura H, Sudhakumari CC,
378 Nagahama Y (2005) Two types of aromatase with diVerent encoding genes, tissue
379 distribution and developmental expression in Nile tilapia (*Oreochromis niloticus*). Gen
380 Comp Endocrinol **141**: 101–115
381 Chaube R, Rawat A, Joy KP (2015) Molecular cloning and characterization of brain and
382 ovarian cytochrome P450 aromatase genes in the catfish *Heteropneustes fossilis*: Sex,
383 tissue and seasonal variation in, and effects of gonadotropin on gene expression. Gen
384 Comp Endocrinol **221**: 120-133
385 Chen H, Zhang Y, Li S, Lin M, Shi Y, Sang Q, Liu M, Zhang H, Lu D, Meng Z, Liu X, Lin H
386 (2011) Molecular cloning, characterization and expression profiles of three estrogen
387 receptors in protogynous hermaphroditic orange-spotted grouper (*Epinephelus coioides*).
388 Gen Comp Endocrinol **172**: 371-381
389 Choi CY, Habibi HR (2003) Molecular cloning of estrogen receptor alpha and expression
390 pattern of estrogen receptor subtypes in male and female goldfish. Mol Cell Endocrinol
391 **204**: 169–177
392 Colin PL, Bell LJ (1991) Aspects of the spawning of labrid and scarid fishes (Pisces:
393 Labroidei) at Enewetak Atoll, Marshall Islands with notes on other families. Env Biol
394 Fish **31**: 229–260
395 Filby AL, Thorpe KL, Tyler CR (2006) Multiple molecular effect pathways of an
396 environmental oestrogen in fish. J Mol Endocrinol **37**: 121–134
397 Halm S, Martínez-Rodrígueza G, Rodrígueza L, Prat F, Mylonas CC, Carrillo M, Zanuy S
398 (2004) Cloning, characterisation, and expression of three oestrogen receptors (ERα,
399 ERβ1 and ERβ2) in the European sea bass, *Dicentrarchus labrax*. Mol Cell Endocrinol
400 **223**: 63–75

401 Hawkins MB, Thornton JW, Crews D, Skipper JK, Dotte A, Thomas P (2000) Identification
402 of a third distinct estrogen receptor and reclassification of estrogen receptors in teleosts.
403 Proc Natl Acad Sci USA **97**: 10751-10756
404 Hojo Y, Hattori TA, Enami T, Furukawa A, Suzuki K, Ishii HT, Mukai H, Morrison JH,
405 Janssen WG, Kominami S, Harada N, Kimoto T, Kawato S (2003) Adult male rat
406 hippocampus synthesizes estradiol from pregnenolone by cytochromes $P450_{17\alpha}$ and P450
407 aromatase localized in neurons. Proc Natl Acad Sci USA **101**: 865–870
408 Hoffman KS, Grau EG (1989) Daytime changes in oocyte development with relation to the
409 tide for the Hawaiian saddleback wrasse, *Thalassoma duperrey.* J Fish Biol **34**: 529–546
410 Holloway CC, Clayton DF (2001) Estrogen synthesis in the male brain triggers development
411 of the avian song control pathway in vitro. Nat Neurosci **4**: 170–175.
412 Hoque MM, Takemura A, Takano K (1998) Annual changes in oocyte development and
413 serum vitellogenin level in the rabbitfish, *Siganus canaliculatus* (Park), in Okinawa,
414 southern Japan. Fisheries Sci **64**: 44–52
415 Huffman LS, O'Connell LA, Hofmann HA (2013) Aromatase regulates aggression in the
416 African cichlid fish *Astatotilapia burtoni*. Physiol Behav **112–113**: 77–83
417 Kazeto Y, Trant JM (2005) Molecular biology of channel catfish brain cytochrome P450
418 aromatase (CYP19A2): cloning, preovulatory induction of gene expression, hormonal
419 gene regulation and analysis of promoter region. J Mol Endocrinol **35**: 571–583
420 Li GL, Liu XC, Lin HR (2007) Seasonal changes of serum sex steroids concentration and
421 aromatase activity of gonad and brain in red-spotted grouper (*Epinephelus akaara*). Anim.
422 Reprod Sci **99**: 156-166
423 Ma CH, Dong KW, Yu KL (2000) CDNA cloning and expression of a novel estrogen
424 receptor beta-subtype in goldfish (*Carassius auratus*). Biochim Biophys Acta **1490**: 145–
425 152.

McEwen BS (1981) Neural gonadal steroid actions. Science **211**: 1303–1311

Matsuyama M., Adachi S, Nagahama Y, Maruyama K, Matsura S (1990) Diurnal rhythm of serum steroid hormone levels in the Japanese whiting, *Sillago japonica,* a daily-spawning teleost. Fish Physiol Biochem **8**: 329–338

Matsuyama M, Morita S, Nasu T, Kashiwagi M (1998) Daily spawning and development of sensitivity to gonadotropin and maturation-inducing steroid in the oocytes of the bambooleaf wrasse, *Pseudolabrus japonicas*. Environ Biol Fish **52**: 281–290

Matsuyama M, Onozato S, Kashiwagi M (2002) Endocrine control of diurnal oocyte maturation in the kyusen wrasse, *Halichoeres poecilopterus*. Zool Sci **19**: 1045-1053

Menuet A, Pellegrini E, Anglade I, Blaise O, Laudet V, Kah O, Pakdel F (2002) Molecular characterization of three estrogen receptor forms in zebrafish: binding characteristics, transactivation properties, and tissue distributions. Biol Reprod **66**: 1881–1892

Mu WJ, Wen HS, Shi D, Yang YP (2013) Molecular cloning and expression analysis of estrogen receptor betas (ERβ1 and ERβ2) during gonad development in the Korean rockfish, *Sebastes schlegeli*. Gene **523**: 39-49

Nagahama Y (1994) Endocrine regulation of gametogenesis in fish. Int J Dev Biol **38**: 217-229

Nagler JJ, Cavileer T, Sullivan J, Cyr DG, Rexroad III C (2007) The complete nuclear estrogen receptor family in the rainbow trout: discovery of the novel *ERα2* and both *ERβ* isoforms. Gene **392**: 164–173

Nagler JJ, Cavileer TD, Verducci JS, Schultz IR, Hook SE, Hayton WL (2012) Estrogen receptor mRNA expression patterns in the liver and ovary of female rainbow trout over a complete reproductive cycle. Gen Comp Endocrinol **178**: 556-561

Nelson ER, Habibi HR (2013) Estrogen receptor function and regulation in fish and other vertebrates. Gen Comp Endocrinol **192**: 15-24

451 Nelson ER, Wiehler WB, Cole WC, Habibi HR (2007) Homologous regulation of estrogen
452 receptor subtypes in goldfish (*Carassius auratus*). Mol Reprod Develop **74**: 1105–1112
453 O'Connell LA, Hofmann HA (2012) Social status predicts how sex steroid receptors regulate
454 complex behavior across levels of biological organization. Endocrinology **153**: 1341–
455 1351.
456 Rasheeda MK, Sridevi P, Senthilkumaran B (2010) Cytochrome P450 aromatases: Impact on
457 gonadal development, recrudescence and effect of hCG in the catfish, *Clarias gariepinus*.
458 Gen Comp Endocrinol **167**: 234–245
459 Ross RM (1983). Annual, semilunar, and diel reproductive rhythms in the Hawaiian labrid
460 *Thalassoma duperrey.* Mar Biol **72**: 311–318
461 Sabo-Attwood T, Kroll KJ, Denslow ND (2004) Differential expression of largemouth bass
462 (*Micropterus salmoides*) estrogen receptor isotypes alpha, beta, and gamma by estradiol.
463 Mol Cell Endocrinol **218**: 107–118
464 Suzuki S, Kuwamura T, Nakashima Y, Karino K, Kohda M (2010) Social factors of group
465 spawning as an alternative mating tactic in the territorial males of the threespot wrasse
466 *Halichoeres trimaculatu*s. Env Biol Fish **89**: 71–77
467 Takemura A, Oya R, Shibata Y, Enomoto Y, Uchimura M, Nakamura S (2008) Role of the
468 tidal cycle in the gonadal development and spawning of the tropical wrasse *Halichoeres*
469 *trimaculatus*. Zool Sci **25**: 572-579
470 Takemura A, Shibata Y, Takeuchi Y, Hur SP, Sugama N, Badruzzaman M (2012) Effects of
471 hydrostatic pressure on monoaminergic activity in the brain of a tropical wrasse,
472 *Halicoeres trimaculatus*: Possible implication for controlling tidal-related reproductive
473 activity. Gen Comp Endocrinol **175**: 173-179

474 Tchoudakova A, Callard GV (1998) Identification of multiple cyp19 genes encoding different
475 cytochrome p450 aromatase isozymes in brain and ovary. Endocrinology **139**: 2179 –
476 2189
477 Tchoudakova A, Kishida M, Wood E, Callard GV (2001) Promoter characteristics of two
478 *cyp19* genes differentially expressed in the brain and ovary of teleost fish. J Steroid
479 Biochem Mol Biol **78**: 427–439
480 Villeneuve DL, Knoebl I, Kahl MD, Jensen KM, Hammermeister DE, Greene KJ, Blake LS,
481 Ankley GT (2006) Relationship between brain and ovary aromatase activity and isoform-
482 specific aromatase mRNA expression in the fathead minnow (*Pimephales promelas*).
483 Aqua Toxicol **76**: 353–368
484 Wallace RA, Selman K (1981) Cellular and dynamic aspects of oocyte growth in teleost.
485 Amer Zool **21**: 325-343
486 Warner RR (1982) Mating systems, sex change and sexual demography in the rainbow wrasse,
487 *Thalassoma lucasanum.* Copeia **1982**: 653–661
488 Zwain IH, Yen SS (1999) Neurosteroidogenesis in astrocytes, oligo-dendrocytes, and neurons
489 of the cerebral cortex of rat brain. Endocrinology **140**: 3843–3852
490

Table 1. Primer sets used for PCR amplification of three-pot wrasse transcripts

Name	Sequence
Cloning for *erα*	
Forward	5'-TGCAGTGACTATGCCTCTGG-3'
Reverse	5'-ATCAGAACCTCAAGCCAGGA-3'
Cloning for *erβ*	
Forward	5'-TCTACATCCCCTCGCCATAC-3'
Reverse	5'-CTTTTACGCCGGTTCTTGTC-3'
Cloning for *cyp19a*	
Forward	5'-AGGCAGTATGTGTTGGAGATGG-3'
Reverse	5'-ACCAGGATGGATTTCTCATCA-3'
Cloning for *cyp19b*	
Forward	5'-GACATGTGGATGCCCTAAATCT-3'
Reverse	5'-AAAGGCTGGAAGAAGCGACT-3'
Cloning for *erα*	
Forward	5'-TCGTCGCCTCAGGAAGTGTTA-3'
Reverse	5'-TCGTACAAGTCCGCCTTTTGT-3'
qPCR for *erβ*	
Forward	5'-AGTCCAAACCCAACAGCATCAG-3'
Reverse	5'-ACCACAGAAGAGCACAACGAGG-3'
qPCR for *cyp19a*	
Forward	5'-TTCTGAACACAGGCCACATGC-3'
Reverse	5'-AAACGGCTGGAAGTAACGACG-3'
qPCR for *cyp19b*	
Forward	5'-TGAAACATGGCAGACGGTTCT-3'
Reverse	5'-ATCACGTCTTGCAGCTCTTGG-3'
qPCR for *β-actin*	
Forward	5'-TACCACCATGTACCCTGGCATC-3'
Reverse	5'-TACGCTCAGGTGGAGCAATGA-3'

Figure legends

Figure 1. Representative view of a brain of the threespot wrasse. The brain of threespot wrasse is divided into three parts: forebrain including telencephalon (TE); midbrain (MB) including optic tectum (OT) and diencephalon (DE); hindbrain (HB) including cerebellum (CE) and medulla oblongata (MO).

Figure 2. Phylogenetic tree of CYP19a and CYP19b in vertebrates. One thousand bootstrap repetitions were performed and values are shown under the nodes. The scale bar is calibrated in substitutions per site. The accession numbers for CYP19a and CYP19b proteins used in the phylogenetic tree analysis are as follows: threespot wrasse *Halichoeres trimaculatus* CYP19a (GenBank accession No. LR35003) and CYP19b (LR35004); Chinese wrasse *H. tenuispinis* CYP19a (AR37048) and CYP19b (AR37047); European seabass *Dicentrarchus labrax* CYP19a (DQ177458) and CYP19b (AY138522); gilthead seabream *Sparus aurata* CYP19a (AF399824); goldfish *Carassius auratus* CYP19a (AB009336) and CYP19b (AB009335); zebrafish *Danio rerio* CYP19a (AF226620) and CYP19b (AF226619); chicken *Gallus gallus* CYP19 (D50335); human *Homo sapiens* CYP19 (AF419338); mouse *Mus musculus* CYP19 (AJ437576); rat *Rattus rattus* CYP19 (EU025135); sheep *Ovis aries* CYP19 (NM001123000).

Figure 3. Phylogenetic tree of ERα and ERβ in vertebrates. One thousand bootstrap repetitions were performed and values are shown on the nodes. The scale bar is calibrated in substitutions per site. The accession numbers for ERα and ERβ proteins used in the phylogenetic tree analysis are as follows: threespot wrasse *Halichoeres trimaculatus* ERα (KT210387) and ERβ (KT210388); Chinese wrasse *H. tenuispinis* ERα (AP72178) and ERβ (AP72179); European seabass *Dicentrarchus labrax* ERα (AJ505009), ERβ1 (AD33851), and ERβ2 (AD33882); gilthead seabream

Sparus aurata ERα (AF136979) and ERβ (AF136980); goldfish *Carassius auratus* ERα (AY055725) and ERβ (AF061269); olive flounder *Paralichthys olivaceus* ERα (AB070629) and ERβ (AB070630); zebrafish *Danio rerio* ERα (AF349412) and ERβ (AF349414); human *Homo sapiens* ERα (NM001122741) and ERβ (AF051427); mouse *Mus musculus* ERα (AB560752) and ERβ (U81451); rat *Rattus rattus* ERα (NM012689) and ERβ (NM012754); sheep *Ovis aries* ERα (AY033393) and ERβ (AF177936).

Figure 4. Changes of gonadosomatic index (a), oocyte diameter (b), and plasma estradiol-17β levels (c) with tidal cycle. Fish (n = 6 – 8 per each point) were collected around points of low tide (LT), flood tide (FT), high tide (HT), and ebb tide (ET). Oocyte diameter of the most developed oocytes (n = 30) on histological slides was calculated in each ovary. Plasma levels of estradiol-17β were measured with enzyme-immunoassay. Each point is expressed as mean ± standard error of the means (SEM). Different letters indicate statistical significance at $P < 0.05$.

Figure 5. Changes in relative mRNA abundance of aromatases *(cyp19a*) and estrogen receptors (*erα* and *erβ*) in the ovary of the threespot wrasse with tidal cycle. Fish (n = 6 – 8 per each point) were collected around points of low tide (LT), flood tide (FT), high tide (HT), and ebb tide (ET). The mRNA abundance of aromatase (a) and estrogen receptors (b) in the ovary was measured qPCR and reported as a ratio with respect to *β-actin*. Each point is expressed as mean ± standard error of the means (SEM). Different letters indicate statistical significance at $P < 0.05$ using a one-way ANOVA followed by LSD-Duncan test.

Figure 6. Changes in relative mRNA abundance of aromatases (*cyp19b*) and estrogen receptors (*erα* and *erβ*) in the brain of the threespot wrasse with tidal cycle. Fish (n = 6 – 8 per each point) were collected around points of low tide (LT), flood tide (FT),

high tide (HT), and ebb tide (ET). The mRNA abundance of *cyp19b* (a, b, and c), *er*α (d, e, and f), and *er*β (g, h, and i) in forebrain (a, d, and g), midbrain (b, e, and h), and hindbrain (c, f, and i) was measured qPCR and reported as a ratio with respect to *β-actin*. Each point is expressed as mean ± standard error of the means (SEM). Different letters indicate statistical significance at $P < 0.05$ using a one-way ANOVA followed by LSD-Duncan test.

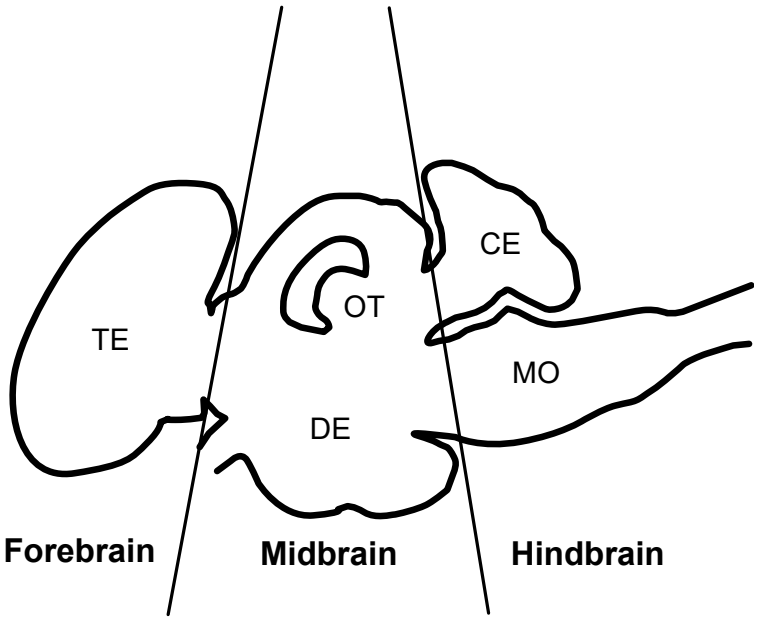

Figure 1

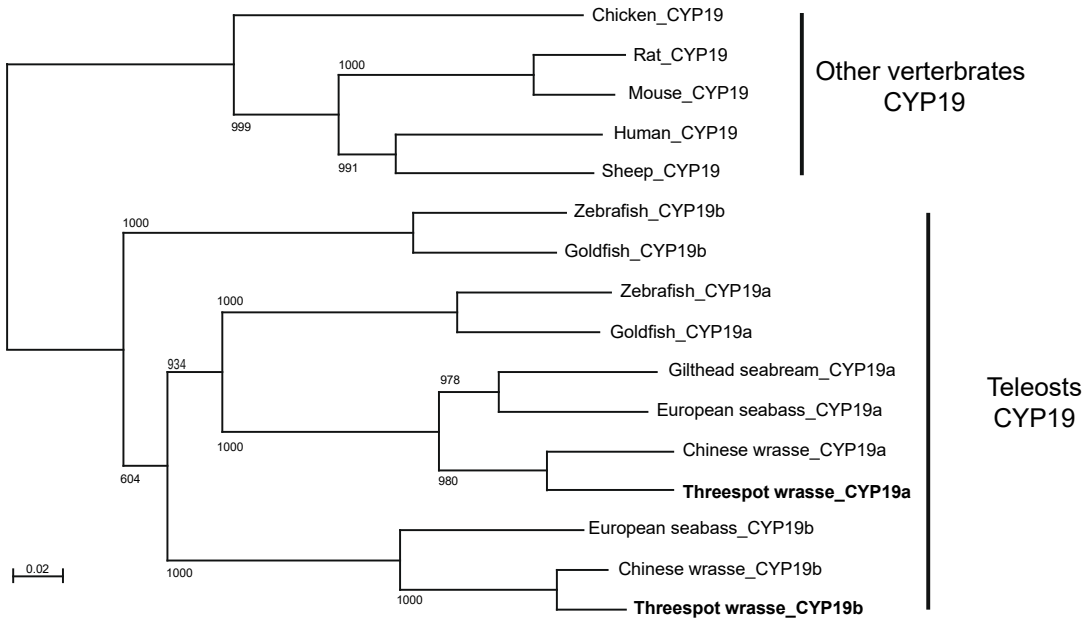
Chicken_CYP19
Rat_CYP19
Mouse_CYP19
Human_CYP19
Sheep_CYP19
1000
999
991
Other verterbrates
CYP19
Zebrafish_CYP19b
Goldfish_CYP19b
Zebrafish_CYP19a
Goldfish_CYP19a
Gilthead seabream_CYP19a
European seabass_CYP19a
Chinese wrasse_CYP19a
Threespot wrasse_CYP19a
European seabass_CYP19b
Chinese wrasse_CYP19b
Threespot wrasse_CYP19b
1000
1000
934
978
1000
604
980
1000
1000
0.02
Teleosts
CYP19

Figure 2

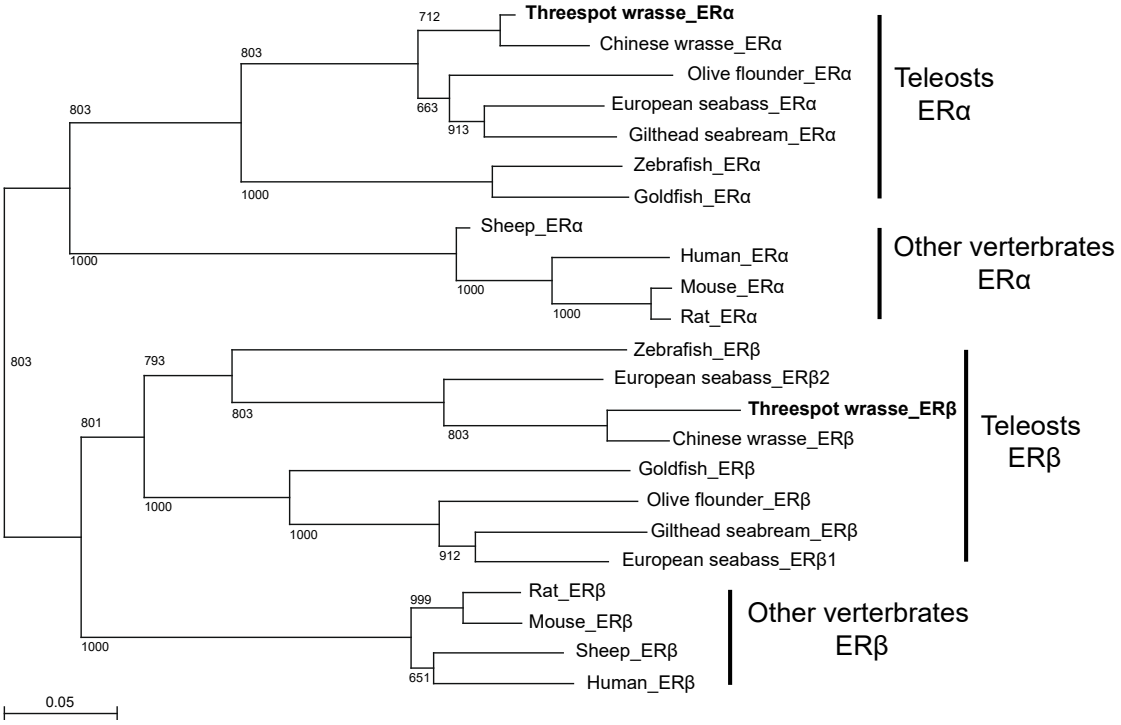
Threespot wrasse_ERα
Chinese wrasse_ERα
Olive flounder_ERα
European seabass_ERα
Gilthead seabream_ERα
Zebrafish_ERα
Goldfish_ERα
Sheep_ERα
Human_ERα
Mouse_ERα
Rat_ERα
Zebrafish_ERβ
European seabass_ERβ2
Threespot wrasse_ERβ
Chinese wrasse_ERβ
Goldfish_ERβ
Olive flounder_ERβ
Gilthead seabream_ERβ
European seabass_ERβ1
Rat_ERβ
Mouse_ERβ
Sheep_ERβ
Human_ERβ
712
803
803
663
913
1000
1000
1000
1000
803
793
803
803
801
1000
1000
912
999
1000
651
0.05
Teleosts ERα
Other verterbrates ERα
Teleosts ERβ
Other verterbrates ERβ

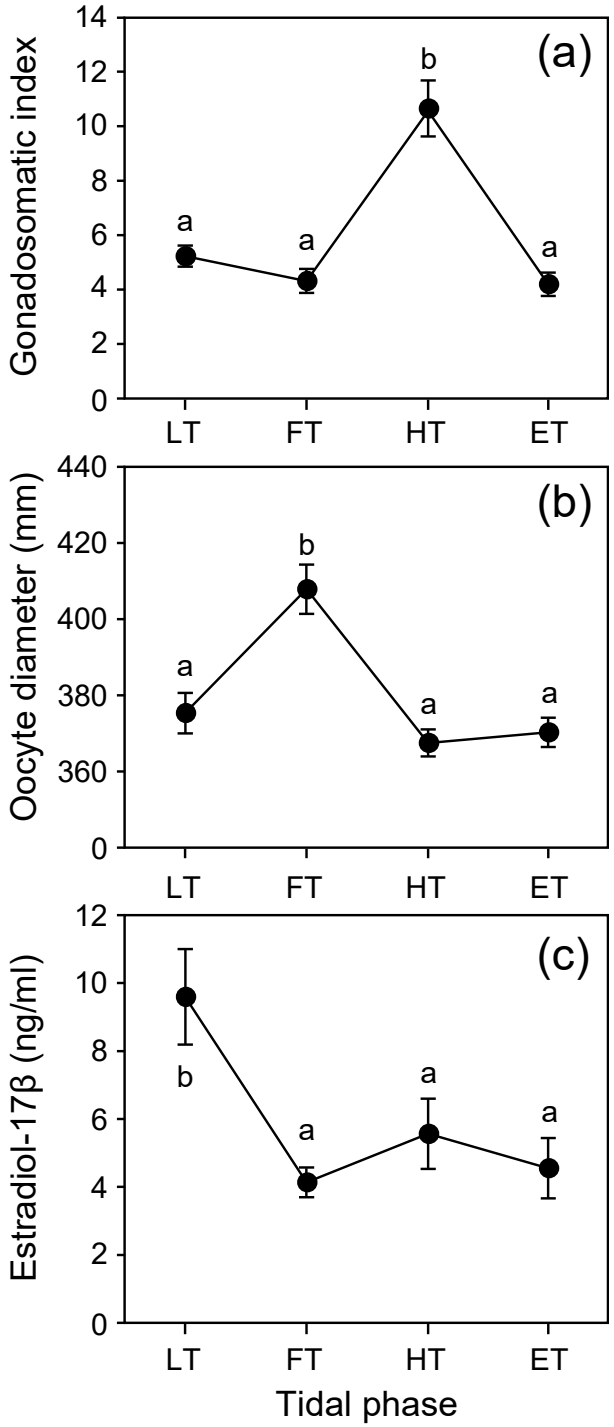
(a)
Gonadosomatic index
14
12
10
8
6
4
2
0
a
a
b
a
LT
FT
HT
ET
(b)
Oocyte diameter (mm)
440
420
400
380
360
0
a
b
a
a
LT
FT
HT
ET
(c)
Estradiol-17β (ng/ml)
12
10
8
6
4
2
0
b
a
a
a
LT
FT
HT
ET
Tidal phase

Figure 4

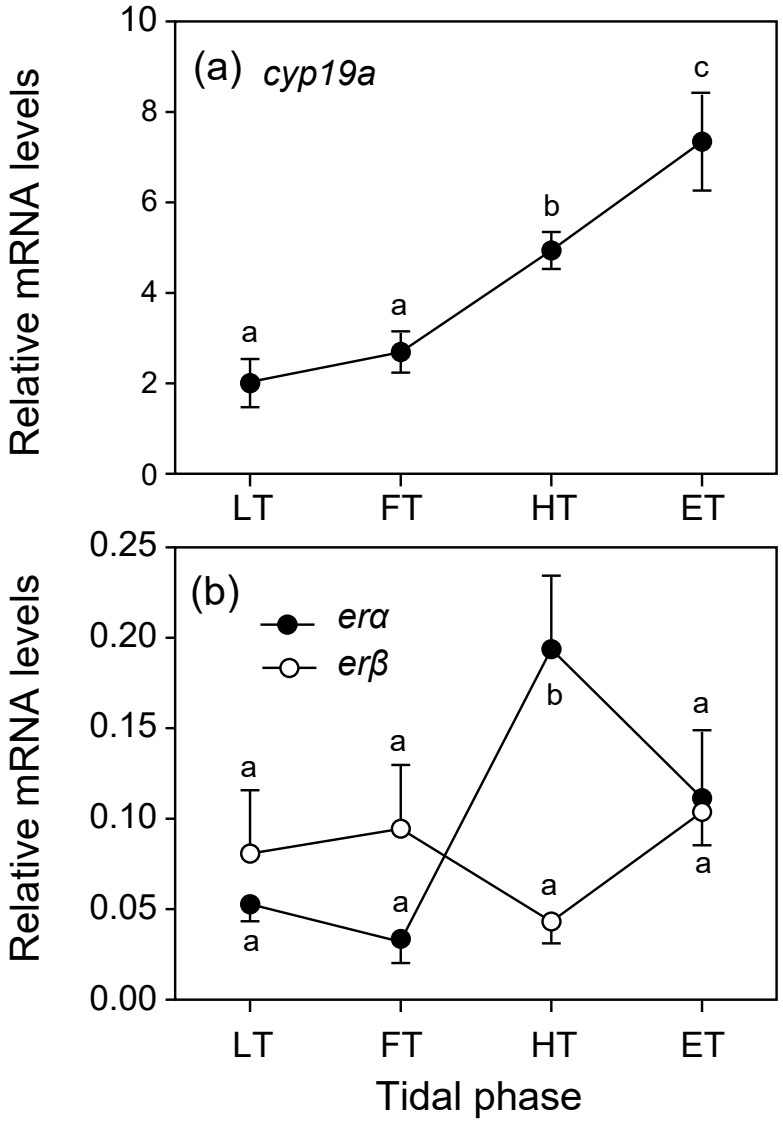
(a) cyp19a
Relative mRNA levels
10
8
6
4
2
0
a
a
b
c
LT
FT
HT
ET
(b)
erα
erβ
Relative mRNA levels
0.25
0.20
0.15
0.10
0.05
0.00
a
a
a
b
a
a
a
a
LT
FT
HT
ET
Tidal phase

Figure 5

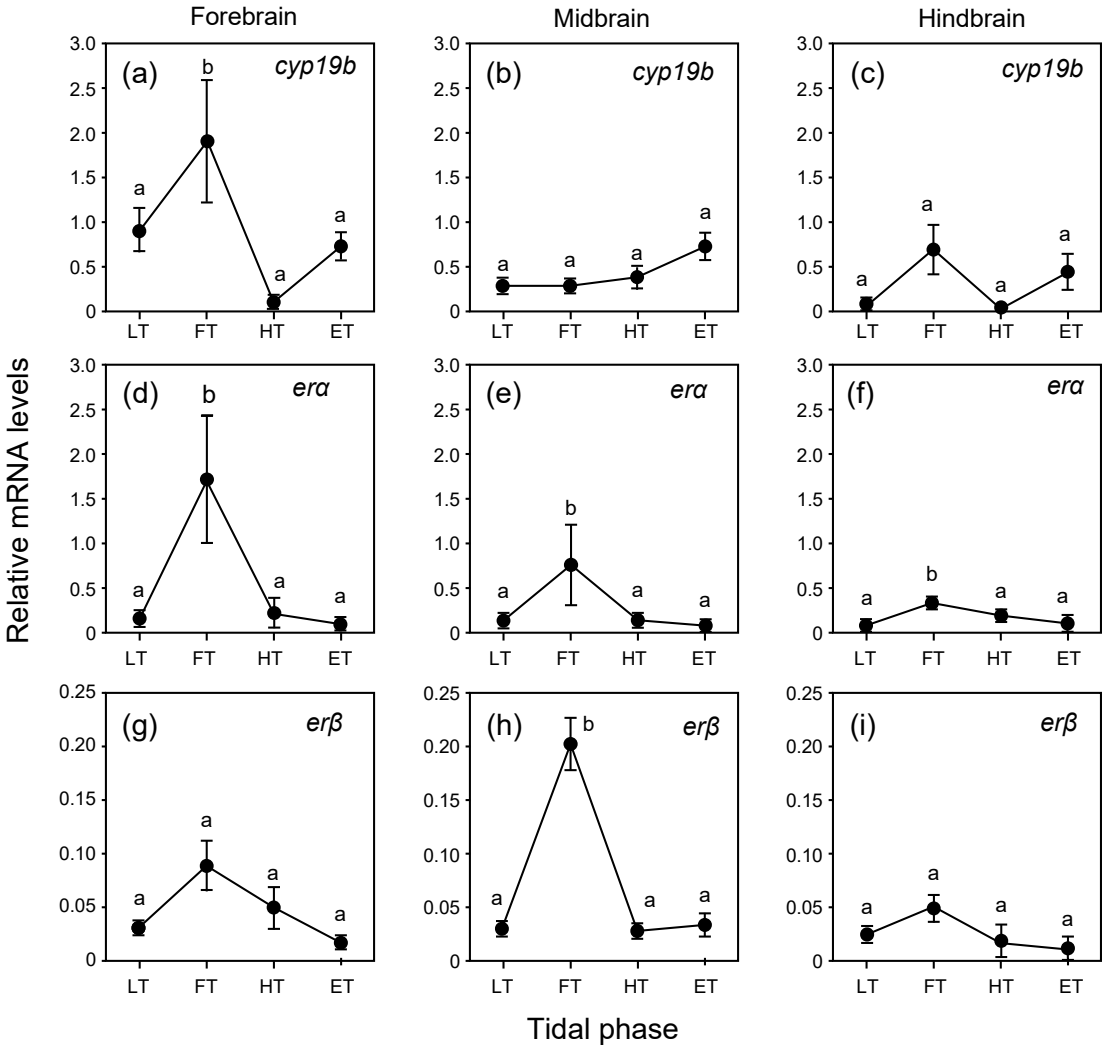
Forebrain
Midbrain
Hindbrain
(a) cyp19b
(b) cyp19b
(c) cyp19b
(d) erα
(e) erα
(f) erα
(g) erβ
(h) erβ
(i) erβ
Relative mRNA levels
Tidal phase
LT
FT
HT
ET

Figure 6